Expression and characterization of recombinant fungal acetyl-CoA carboxylase and isolation of a soraphen-binding domain

Stephanie C. WEATHERLY[1], Sandra L. VOLRATH[1] and Tedd D. ELICH[2]
Cropsolution, Inc., P.O. Box 14069, Research Triangle Park, NC 27560, U.S.A.

Acetyl-CoA carboxylase (ACC) catalyses the first step in fatty-acid biosynthesis. Owing to its role in primary metabolism, ACC has been exploited as a commercial herbicide target and identified as a chemically validated fungicide target. In animals, ACC is also a key regulator of fat metabolism. This function has made ACC a prime target for the development of anti-obesity and anti-Type II diabetes therapeutics. Despite its economic importance, there is a lack of published information on recombinant expression of ACC. We report here the expression of enzymically active fungal (*Ustilago maydis*) ACC in *Escherichia coli*. The recombinant enzyme exhibited K_m values of 0.14 ± 0.013 mM and 0.19 ± 0.041 mM for acetyl-CoA and ATP respectively, which are comparable with those reported for the endogenous enzyme. The polyketide natural product soraphen is a potent inhibitor of the BC (biotin carboxylase) domain of endogenous fungal ACC. Similarly, recombinant ACC activity was inhibited by soraphen with a K_i of 2.1 ± 0.9 nM. A truncated BC domain that included amino acids 2–560 of the full-length protein was also expressed in *E. coli*. The isolated BC domain was expressed to higher levels, and was more stable than full-length ACC. Although incapable of enzymic turnover, the BC domain exhibited high-affinity soraphen binding (K_d 1.1 ± 0.3 nM), demonstrating a native conformation. Additional BC domains from the phytopathogenic fungi *Magnaporthe grisea* and *Phytophthora infestans* were also cloned and expressed, and were shown to exhibit high-affinity soraphen binding. Together, these reagents will be useful for structural studies and assay development.

Key words: acetyl-CoA carboxylase, biotin carboxylase, biotin carboxylase inhibitor, fungicide, soraphen.

INTRODUCTION

ACC catalyses the conversion of acetyl-CoA into malonyl-CoA, which is the first committed step in fatty-acid biosynthesis. ACC is a multifunctional enzyme in that this conversion is accomplished via sequential half-reactions: the ATP-dependent carboxylation of enzyme-bound biotin followed by the transfer of the carboxy group to acetyl-CoA. The BC (biotin carboxylase), BCCP (biotin carboxyl carrier protein) and CT (carboxyltransferase) functions are contained on a single, large ($\approx$250 kDa) multidomain polypeptide in the ACCs found in animals, fungi, plant cytosols, and the plastids of grasses (referred to as eukaryotic ACCs). In contrast, these functions reside on separate protein subunits in the ACCs found in bacteria and the plastids of most plants, except grasses (referred to as prokaryotic ACCs) [1,2].

ACC is a current agrochemical target and a potential pharmaceutical target. Two classes of commercial herbicides, the aryloxyphenoxypropionates and the cyclohexanediones, inhibit the CT function of the eukaryotic ACCs found in the plastids of grasses [3]. Additionally, ACC is the target of the fungicidal polyketide soraphen, which is produced by the myxobacterium *Sorangium cellulosum* [4]. Unlike the herbicide mode of action, however, soraphen is a potent inhibitor of the BC domain [5–7]. Finally, ACC is under investigation as a pharmaceutical target, since appropriate inhibitors could serve as treatments for obesity [8,9], Type II diabetes [9,10] and microbial infections [11].

Despite its economic importance, detailed knowledge about ACC structure and molecular interactions with known inhibitors is lacking. Crystal structures are currently available only for the BC and BCCP subunits of the *Escherichia coli* enzyme [1], and for an isolated CT domain of *Saccharomyces cerevisiae* ACC [12]. At present, there are no published structures of either eukaryotic or prokaryotic ACCs with bound inhibitors. One reason for the paucity of structural information is the difficulty in obtaining sufficient quantities of pure protein. Eukaryotic ACCs are difficult to purify in quantity from endogenous sources, and their size and complexity make recombinant expression difficult as well. In this regard, we are aware of only one report of the recombinant expression of a full-length eukaryotic ACC; however, the *Toxoplasma gondii* ACC expressed in that study was extensively proteolysed, the bulk of it lacked bound biotin, and the preparation had very low specific activity [11].

Here, we report the high-level recombinant expression of active full-length fungal (*Ustilago maydis*) ACC in *E. coli*. The recombinant enzyme is characterized in terms of its kinetic properties, biotinylation and inhibition by soraphen. In addition, we report the isolation and expression of small and stable soraphen-binding domains derived from the BC region of ACC.

EXPERIMENTAL

Chemicals

Sodium [^{14}C]bicarbonate (48.7 mCi/mmol) was obtained from PerkinElmer Life Sciences. Soraphen A was acquired from Professor Gerhard Hoefle (The German Research Centre for

Abbreviations used: (r)ACC, (recombinant) acetyl-CoA carboxylase; (r)BC, (recombinant) biotin carboxylase; BCCP, biotin carboxyl carrier protein; CT, carboxyltransferase; DTT, dithiothreitol; IPTG, isopropyl β-D-thiogalactoside; K_m (app), apparent K_m; Ni-NTA, Ni^{2+}-nitrilotriacetate; $rBC_{M.g.}$, the rBC domain from the *M. grisea* ACC; $rBC_{P.i.}$, the rBC domain from *P. infestans* ACC; SEC, size-exclusion chromatography.

[1] These authors contributed equally to this work.

[2] To whom correspondence should be addressed (e-mail telich@cropsolution.com).

Biotechnology, Braunschweig, Germany). [^{3}H]Soraphen A (3.65 Ci/ mmol) was produced by Sibtech, Inc. (Newington, CT, U.S.A.) using a proprietary tritiation procedure, and was stored as a 96.2 μM stock in ethanol at -20 °C. All other chemicals were reagent grade.

Cloning of full-length ACC and BC domains

Genomic DNA from *U. maydis* strain 1/2 [13] was provided by Dr Scott Gold (University of Georgia, Athens, GA, U.S.A.). Primers derived from GenBank® accession number Z46886 were used to PCR-amplify the full-length *U. maydis* ACC-coding region from genomic DNA. The 5′-primer included an *Nde*I site (5′-CAT ATG CCG CCT CCG GAT CAC AAG GC-3′); the 3′-primer included a *Not*I site (5′-GCG GCC GCC TTG AGC GAA GCG GCT AG-3′; the two restriction sites here for *Nde*I and *Not*I, and those that follow subsequently for other restriction endonucleases, are shown underlined). The single 80 bp intron was deleted using overlapping PCR to join the two exons, generating a complete cDNA clone. The cDNA sequence corresponded to the GenBank® clone, with the exception of three adjacent base changes that convert Ala-Ala into Gly-Thr at amino acid positions 472 and 473. These changes were observed in multiple independent clones, and were confirmed in the sequence subsequently released by the *U. maydis* genome project (Fungal Genome Initiative; http://www.broad.mit.edu/annotation/fungi/fgi/index.html). The full-length ACC cDNA was ligated into *Nde*I/*Not*I-digested pET30a (Novagen, Madison, WI, U.S.A.) to create pCS11, encoding C-terminal His_6-tagged recombinant (r)ACC.

The BC region of *U. maydis* ACC was identified on the basis of sequence similarity to the BC subunit of *E. coli* ACC (GenBank® accession no. M80458). This domain was amplified with a 5′-primer containing a *Bam*HI site (5′-GGA TCC CCG CCT CCG GAT CAC AAG-3′) and a 3′-primer containing a *Hin*dIII site plus two stop codons (5′-AAG CTT ACT AGA CAG CGA GGT CCG CAG GA-3′). The PCR product was ligated into *Bam*HI/*Hin*dIII-digested pET28a (Novagen) to create pCS8, encoding N-terminal His_6-tagged recombinant (r)BC.

Genomic DNA from the phytopathogenic fungus *Magnaporthe grisea*, strain Guy11 [14], was provided by Dr Jin-Rong Xu (Purdue University, West Lafayette, IN, U.S.A.). PCR primers were designed from the first-draft sequence released by the *M. grisea* genome project (Fungal Genome Initiative, http://www.broad.mit.edu/annotation/fungi/fgi/index.html), using alignment to the *U. maydis* ACC and splice-site consensus sequences to predict the coding region for the BC domain. The 5′-primer included a *Bam*HI site (5′-GGA TCC ACT GAG ACA AAT GGA ACC-3′) and the 3′-primer included a *Not*I site and two stop codons (5′-GCG GCC GCT ATT AAA CAG CAA GCA TCT TGT CGG-3′). One predicted 70 bp intron was removed by overlapping PCR fusion, and the resulting cDNA fragment was cloned into *Bam*HI/*Not*I-digested pET28a to create pCS17, encoding N-terminal His_6-tagged $rBC_{M.g.}$ (the rBC domain from the *M. grisea* ACC).

Genomic DNA from the phytopathogenic fungus *Phytophthora infestans*, genotype US-1, was provided by Dr Jean Ristaino (North Carolina State University, Raleigh, NC, U.S.A.). Primers for PCR were designed from EST (expressed sequence tag) sequences published by the Phytophthora Genome Consortium (https://xgi.ncgr.org/pgc/). The 5′-primer (5′-CAA AAT ATG GTG GCC GAG GAA GC-3′) was derived from CON 001 05979, and the 3′-primer (5′-TTC GAA CGA GCC AGC TTC GAC GC-3′) was derived from CON 001 08387. The amplification product was approx. 4970 bp, and encoded the N-terminal portion of the *P. infestans* ACC. This fragment was sequenced, and additional primers were designed for specific amplification of the BC domain. The 5′-primer included an *Nde*I site (5′-CAT ATG GTG GCC GAG GAA GCG-3′), and the 3′-primer included a *Hin*dIII site (5′-AAG CTT GTC CGG CCG ACC CTG TAG-3′). The PCR product was ligated into *Nde*I/*Hin*dIII-digested pET30a to create pCS15, encoding C-terminal His_6-tagged $rBC_{P.i.}$ (the rBC domain from *P. infestans* ACC). The *P. infestans* BC domain sequence was deposited as GenBank® accession no. AY444507.

Protein expression and purification

All expression constructs were transformed into *E. coli* strain BL21(DE3) (Novagen). Transformants were grown in LB (Luria–Bertani) media containing 50 μg/ml kanamycin to a D_{590} of 0.5–0.6, before induction. Cells were induced with 0.2 mM IPTG (isopropyl β-D-thiogalactoside) for 16 h at 18 °C, harvested and frozen at -80 °C. For pCS11 cultures, 10 μg/ml D-biotin (Sigma, St Louis, MO, U.S.A.) was added with the IPTG.

The cell pellets were broken open by sonication and the recombinant proteins were purified on Ni-NTA (Ni^{2+}-nitrilotriacetate) His-Bind resin (Novagen), as described by the manufacturer, except that 1 % (v/v) protease-inhibitor cocktail (Sigma cat. no. P8849) was added to all buffers. An equal volume of saturated ammonium sulphate was added to the fractions eluted from the Ni-NTA resin, and the protein precipitates were collected by centrifugation at 12 000 ***g*** for 15 min. The pellets were resuspended in storage buffer [200 mM sodium phosphate (pH 7.0)/10 % (v/v) glycerol], clarified by centrifugation at 100 000 ***g*** for 15 min, and stored at -80 °C. Protein concentrations were determined with Coomassie Plus Protein Assay Reagent (Pierce) using BSA as the standard. SDS/PAGE analysis of proteins was performed using 4–20 % Criterion Precast Gels (Bio-Rad) and All Blue Precision Plus Protein Standards (Bio-Rad), according to the manufacturer's instructions.

Enzyme assays

The [^{14}C]bicarbonate incorporation assay was performed essentially as described previously [15]. The reaction mixture (200 μl) contained 50 mM Hepes, pH 8, 2.5 mM $MgCl_2$, 1 mM ATP, 0.5 mM DTT (dithiothreitol), 10 mM $NaHCO_3$, 0.95 mM $NaH^{14}CO_3$ (48.7 mCi/mmol), 0.03 % (v/v) DMSO and $\approx$3–9 μg of purified rACC. After pre-incubation at 30 °C for 10 min, acetyl-CoA was added to a final concentration of 0.33 mM to start the reaction. After 10 min at 30 °C, the reaction was stopped by transferring 150 μl aliquots to glass vials containing 40 μl of concentrated HCl. The samples were evaporated by heating at 70 °C, and then resuspended in 250 μl of H_2O. For quantification of incorporated label, the samples were counted after addition of 3 ml of scintillation fluid. For TLC analysis, the reaction mixture was spotted on to K_{18}CF plates (Whatman) and chromatographed alongside a malonyl-CoA standard using a 50 % acetonitrile mobile phase. The [^{14}C]malonyl CoA product was detected by phosphorimaging.

The spectrophotometric assay was performed essentially as described previously [16]. The reaction mixture (200 μl volume) contained 50 mM Hepes, pH 8, 2.5 mM $MgCl_2$ {except that 10 mM $MgCl_2$ was used for apparent K_m [K_m (app)] determinations}, 0.5 mM phosphoenolpyruvate, 0.2 mM NADH, 1.1 units of pyruvate kinase, 2.3 units of lactate dehydrogenase, 11 mM $NaHCO_3$, 1 mM ATP, 0.5 mM DTT, 0.03 % (v/v) DMSO and $\approx$3 μg of purified ACC. The mixture was separated into aliquots into microtitre plate wells, mixed and pre-incubated for 10 min at 30 °C. The reaction was started by addition of acetyl-CoA to a final concentration of 0.33 mM. The time-dependent

decrease in 340 nM absorbance was monitored, and used to calculate initial reaction velocities.

For determination of K_m (app) values for acetyl-CoA and ATP, the concentration of the substrate under investigation was varied under the conditions described above, and the data were fitted to standard Michaelis–Menten equations using non-linear regression [17]. Two independent determinations, with 8–11 data points per experiment, were performed for each substrate (mean ± range values are reported in Table 1). The 95 % confidence intervals for the fits ranged from 15 % to 30 % of the determined K_m (app) values.

For soraphen inhibition experiments, the mixtures were pre-incubated with various concentrations of soraphen for 10 min at 30 °C, before adding acetyl-CoA to start the reaction. For determination of K_i (app) values, the initial velocity data were fitted to the Morrison equation for tight binding inhibitors [18] using non-linear regression, as described previously [19]. Three independent determinations were performed (mean ± S.D. values reported in Table 1), and the 95 % confidence intervals for the fits ranged from 86 % to 507 % of the determined K_i (app) values. Note that for a non-competitive inhibitor like soraphen, K_i (app) = K_i, assuming that the inhibitor binds similarly to the enzyme and enzyme–substrate complex.

Soraphen binding assay

Various concentrations of [^{3}H]soraphen were incubated with test proteins (5–10 nM) in PNT buffer [100 mM sodium phosphate (pH 7.0)/150 mM NaCl/0.01 % (v/v) Triton X-100] at 25 °C for 45 min. Aliquots (0.5 ml) were applied to PNT-equilibrated NAP-5 columns (Amersham Biosciences). NAP-5 columns contain Sephadex G-25, which has an exclusion limit of 5000 Da; therefore protein-bound soraphen was separated from free soraphen by rapid elution with 1 ml of PNT. The bound [^{3}H]soraphen in the eluted fraction was quantified by liquid scintillation counting. K_d values were determined by fitting the data to an equation for single-site saturation binding with ligand depletion [17]. The non-specific-binding factor was determined empirically by repeating the experiment in the presence of excess unlabelled soraphen [17]. Experiments with rACC and rBC were repeated three and four times respectively. The 95 % confidence intervals for each fit ranged from 61–113 % (rACC) and 33–135 % (rBC) of the determined K_d values.

Dissociation experiments were performed by incubating 53.6 pmol of rBC with 30 pmol of [^{3}H]soraphen in 2 ml of PNT buffer for 15 min. The protein with bound [^{3}H]soraphen was separated from free [^{3}H]soraphen using four NAP5 columns, as described above. The eluates were combined (4 ml total volume), and unlabelled soraphen was added to a final concentration of 2 μM. Soraphen dissociation was followed by removing 0.5 ml aliquots at various times and applying them to NAP5 columns to again separate bound from free label. The bound [^{3}H]soraphen in the eluates was quantified by scintillation counting, and the dissociation rate constant (k_{off}) was determined by fitting the data to the following equation: $Y = Y_{max} \cdot e^{-kt} + B$ (where B is the bottom asymptote representing non-specific binding).

SEC (size-exclusion chromatography)

Experiments were performed at 4 °C on a Duo-Flow Liquid Chromatography System (Bio-Rad) using a Bio-Silect SEC 250–5 column (Bio-Rad) and a mobile phase [100 mM sodium phosphate buffer (pH 7.0)/150 mM NaCl] at a flow rate of 1 ml · min^{-1}. The column was calibrated using Bio-Rad Gel Filtration Standards (#151-1901).

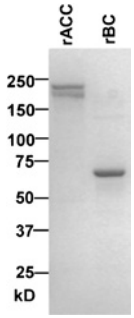

Figure 1 SDS/PAGE analysis of purified proteins

Coomassie Blue-stained SDS-polyacrylamide gel of 1 μg of purified rACC and rBC.

Biotinylation assay

Samples (50 μl) containing 0.1–45 ng of MBP-AviTag fusion protein (a fully biotinylated positive control; Avidity, L.L.C.) or pCS11 protein were adsorbed onto the wells of a flat bottom polystyrene microtitre plate. The plate was washed with PBST buffer [PBS + 0.05 % (v/v) Tween 20] and blocked with 40 mg/ml BSA in PBS. After another PBST wash, the plate was incubated with streptavidin–alkaline phosphatase. After a final wash with TBS, the assay was developed with *p*-nitrophenyl phosphate. The reaction was stopped by the addition of 2 M KOH, and A_{405} was read with a plate reader. The slopes from plots of A_{405} against pmol of protein were determined and compared.

RESULTS AND DISCUSSION

Expression of rACC

A full-length synthetic *U. maydis* ACC cDNA was constructed and cloned into pET30a to create expression construct pCS11. rACC, encoded by pCS11, is expressed as a fusion protein with a C-terminal His_6-tag to facilitate purification. Preliminary studies indicated that virtually all of the rACC expressed from pCS11 under standard induction conditions (1 mM IPTG at 37 °C for 2–3 h) was insoluble. By performing overnight induction with 0.2 mM IPTG at 18 °C, the amount of soluble rACC was increased to ≈ 10 % of the total. Purification of this soluble fraction by Ni-NTA chromatography yielded an average of 6.9 mg of rACC per litre of culture. For comparison, purification of the endogenous enzyme was reported to yield 12 mg of protein/100 litres of *U. maydis* fermentation culture [7].

The predicted molecular mass of rACC is 241.4 kDa, whereas SDS/PAGE analysis of the purified protein demonstrated both a major and a minor product, running at 225 and 190 kDa respectively (Figure 1). Both products must have an intact C-terminus, since they are purified by virtue of a C-terminal His_6-tag; therefore the 190 kDa band is likely to result from N-terminal proteolysis of the 225 kDa band. Additional smaller fragments were sometimes observed, consistent with protease susceptibility. Attempts to reduce the observed proteolysis with modified procedures and other protease inhibitors were unsuccessful. Protease susceptibility of rACC has been observed previously [11]. The discrepancy in size between the 225 kDa band and the predicted 241 kDa molecular mass of the full-length protein is probably due to SDS-gel sizing artifacts, rather than additional truncations. This conclusion is based on the fact that highly conserved portions of the eukaryotic BC domain begin at residue 35 of the *Ustilago* sequence, and a 100 % conserved serine corresponding to residue 57 in the *Ustilago* sequence has been shown to be required for

Table 1 Summary of physical and kinetic properties

Data for the endogenous *U. maydis* ACC are taken from [7]; those for rACC and rBC are from the present study (the number of independent experiments is shown in parentheses). ND, not determined; N/A, not applicable.

Physical/kinetic property	Endogenous *U. maydis* ACC	rACC	rBC
Predicted molecular mass (kDa)	240.0	241.4	64.7
Molecular mass determined by SDS/PAGE (kDa)	200	225	65
Molecular mass determined by native SEC (kDa)	ND	880	66
Specific activity (μmol · min^{-1} · mg^{-1})	12.9	0.3 ± 0.09 (6)	N/A
K_m (app) for acetyl-CoA (mM)	0.08 ± 0.03	0.14 ± 0.02 (2)	N/A
K_m (app) for ATP (mM)	0.39 ± 0.13	0.19 ± 0.04 (2)	N/A
K_i for soraphen (nM)	1.4 ± 0.08	2.1 ± 0.9 (3)	N/A
K_d for soraphen (nM)	ND	0.8 ± 0.3 (3)	1.1 ± 0.3 (4)

soraphen inhibition in yeast [6]. Therefore, although we cannot rule out small N-terminal truncations of our major product, we conclude that truncations larger than ≈3–6 kDa would result in inactive protein that would not bind soraphen.

SEC analysis of the purified product led to an estimation of the molecular mass of approx. 880 kDa (see Table 1 for a summary of data). This result suggests that the native enzyme exists as a tetramer, as has been reported for purified yeast ACC [20]. In contrast, a recombinant CT domain derived from yeast ACC was reported to be a dimer [12]. Furthermore, eukaryotic ACCs purified from plants and animals are also reported to be dimers [3,21,22]. It should be noted that ACCs from animals are known to undergo polymerization events that are thought to be involved in enzyme activation [21,22]. Therefore it is possible that the protomeric form of fungal ACC is a dimer, and that the tetramers observed in the present study (and in [20]) are the result of subsequent association events.

rACC activity

Purified rACC was demonstrated to be enzymically active using a [^{14}C]bicarbonate incorporation assay. In this assay, activity is determined by counting acid- and heat-stable ^{14}C, following incubation of the enzyme with ATP, acetyl-CoA and [^{14}C]bicarbonate. Controls demonstrated that ^{14}C-incorporation was dependent on the presence of both acetyl-CoA and rACC (Figure 2A). Additionally, TLC analysis verified that the counts were incorporated into malonyl-CoA by demonstrating co-migration with an unlabelled standard (Figure 2A).

ACC requires a covalently bound biotin prosthetic group for activity. The fact that rACC was active demonstrated that at least some of the enzyme was biotinylated by the *E. coli* biotin protein ligase. However, the high level of expression that we achieved raised concerns that we might be exceeding the biotinylation capacity of the cells. Consistent with this concern, preliminary studies demonstrated that addition of 10 μg/ml biotin to the bacterial culture during rACC induction resulted in an ≈65 % increase in the specific activity of the purified product. Additional exogenous biotin did not result in further increases, suggesting that biotin was no longer limiting; however, it was still possible that we exceeded the capacity of the endogenous biotin protein ligase. To test this, we directly assessed the extent of rACC biotinylation using streptavidin-conjugated alkaline phosphatase in a plate-based colorimetric assay. The results confirmed that

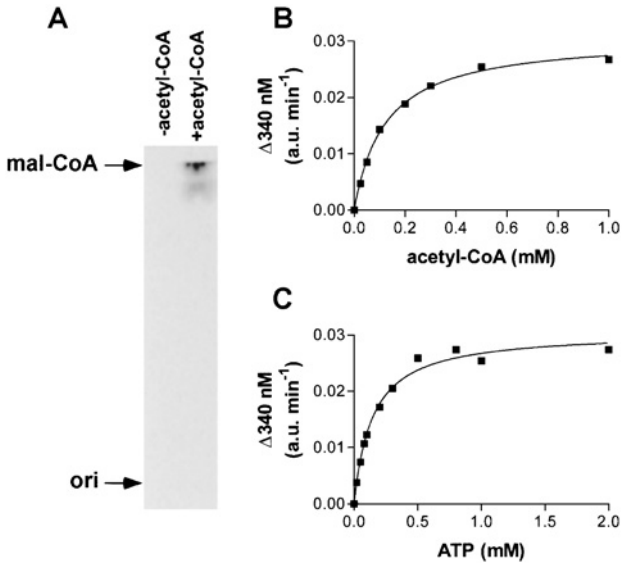

Figure 2 Enzymic activity of rACC

(**A**) Phosphorimage of TLC analysis of products from a [^{14}C]bicarbonate incorporation assay of rACC in the absence (−) and presence (+) of acetyl-CoA. ori, origin. (**B**) Initial-velocity measurements plotted against [acetyl-CoA] from the spectrophotometric assay; a non-linear regression fit of these data to standard Michaelis–Menten kinetics estimated a K_m (app) of 0.12 ± 0.02 mM (± 95 % confidence interval). (**C**) Initial-velocity measurements plotted against [ATP] from the spectrophotometric assay; a non-linear regression fit of these data to standard Michaelis–Menten kinetics estimated a K_m (app) of 0.15 ± 0.04 nM (± 95 % confidence interval).

exogenous biotin during induction increased rACC biotinylation, and demonstrated that the resulting rACC responded similarly to a fully biotinylated control protein on a molar basis (results not shown, also see the Experimental section). This indicates that our standard rACC preparations contain approximately equimolar levels of biotin. In contrast, only ≈2.5 % of recombinant *T. gondii* ACC was reported to be biotinylated [11].

For further enzymic analysis of rACC, we employed a continuous spectrophotometric assay that couples the production of ADP with the oxidation of NADH. Using this assay, we determined the K_m (app) values for acetyl-CoA and ATP to be 0.14 ± 0.02 mM and 0.19 ± 0.04 mM respectively (mean ± range, $n = 2$; representative experiments are shown in Figures 2B and 2C). These values are in reasonable agreement with those of 0.08 ± 0.03 mM and 0.39 ± 0.13 mM reported for endogenous *U. maydis* ACC [7]. Since slightly different standard conditions were used in the two studies, exact agreement of K_m (app) values was not necessarily expected.

The specific activity of our purified rACC averaged 0.3 ± 0.09 μmol · min^{-1} · mg^{-1} (mean ± S.D., $n = 6$). Although this is > 1800-fold greater than that reported for the recombinant *T. gondii* enzyme [11], it is significantly lower than values reported for purified endogenous fungal ACCs. For example, specific activities of 12.9 μmol · min^{-1} · mg^{-1}, 6–9 μmol · min^{-1} · mg^{-1} and 8 μmol · min^{-1} · mg^{-1} were reported for the *U. maydis* [7], yeast [20] and *Candida lipolytica* [23] enzymes respectively. This suggests that our preparations contained non-functional protein. Consistent with this, we observed that ≈15–25 % of the purified rACC was eluted in the void volume during SEC analysis, indicative of misfolded soluble aggregates. Additionally, the major ≈190 kDa proteolytic product, typically comprising 25–50 % of the total rACC, is probably inactive, since it presumably is missing substantial portions of the conserved BC domain. Even

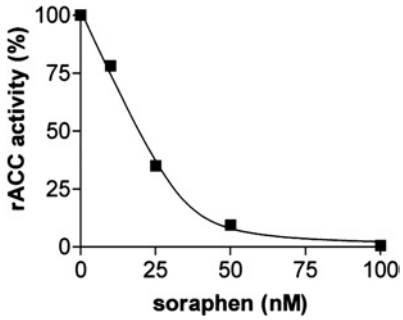

Figure 3 Soraphen inhibition of rACC activity

Representative experiment showing soraphen inhibition of rACC activity. A non-linear regression fit of these data to the Morrison equation for tight binding inhibitors estimated a K_i (app) of 1.5 ± 1.3 nM ($\pm$ 95 % confidence interval).

so, aggregation and proteolysis do not appear to account fully for the 20–40-fold lower specific activity, since we estimated that 25–60 % of our preparations consisted of full-length, properly folded and fully biotinylated protein. However, if each monomer of a holoenzyme must be functional for activity, as has been reported for the *E. coli* BC subunit [24], then the observed aggregation and proteolysis could explain the low specific activity of rACC (i.e. in such a situation, preparations containing $\approx$25 % competent monomers would only exhibit $\approx$6 % active dimers).

Soraphen inhibition of rACC

The macrocyclic polyketide soraphen has fungicidal activity and acts by inhibiting the BC domain of ACC [4–7]. Soraphen was reported to be a non-competitive inhibitor of wild type *U. maydis* ACC, with a K_i of 1.4 ± 0.08 nM [7]. Similarly, soraphen inhibited rACC activity with a K_i of 2.1 ± 0.9 nM (mean $\pm$ S.D., $n = 3$; a representative experiment is shown in Figure 3). We also prepared [^{3}H]soraphen and developed a saturation binding assay. In this assay, rACC was shown to bind [^{3}H]soraphen with a K_d of 0.8 ± 0.3 nM (mean $\pm$ S.D., $n = 3$; a representative experiment is shown in Figure 4A), in excellent agreement with the K_i measurement.

Expression of a soraphen-binding BC domain

One of our primary interests is understanding the molecular interactions between ACC and known inhibitors in order to provide a foundation for the identification of novel inhibitors. In some cases, isolated domains can be more stable than full-length proteins, and thus are better suited for crystallization studies and assay development. For example, the expression and structural determination of an isolated CT domain from yeast ACC was recently reported [12]. Since soraphen is the most potent ACC inhibitor known and it acts by inhibiting the BC domain of ACC [5,6], we concentrated on expressing truncated polypeptides encompassing this region in order to identify a soraphen-binding domain.

We identified the BC region of rACC on the basis of similarity to the BC subunit of *E. coli* ACC (GenBank® accession no. M80458). We then tested 63 different constructs incorporating this region for soluble protein expression. These constructs differed in their purification tag, the position of the tag (N- or C-terminus) and their length. Construct pCS8 encodes an N-terminal His_6-tagged protein containing residues 2–560 of *U. maydis* ACC. Approx. 50 % of the total rBC domain expressed by pCS8 was soluble. Purification of soluble rBC by Ni-NTA chromatography

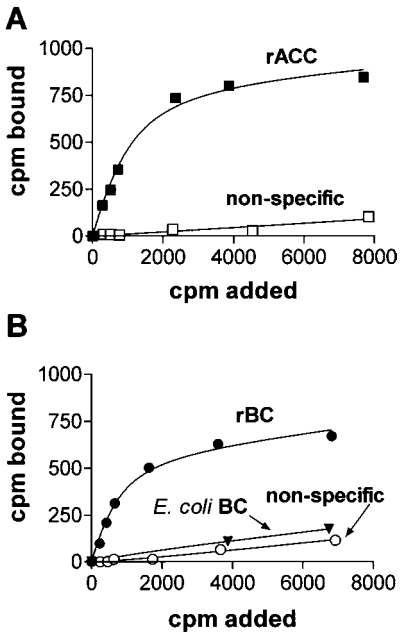

Figure 4 Soraphen binding assays

Representative [^{3}H]soraphen saturation binding assays of rACC (**A**) and rBC (**B**). Non-specific binding was determined by repeating the experiment in the presence of 1 μM unlabelled soraphen. A lack of soraphen binding by *E. coli* BC is also shown (**B**). Non-linear regression fits of these data to an equation for standard one-site saturation binding with ligand depletion gave estimates of 1.2 ± 0.7 nM and 0.9 ± 0.5 nM for the K_d values of rACC and rBC respectively ($\pm$ 95 % confidence interval).

yielded $\approx$25 mg per litre of culture. The predicted molecular mass of rBC is 64.7 kDa, and the purified product ran as a single 65 kDa polypeptide on SDS/PAGE (Figure 1). SEC analysis of rBC under native conditions yielded a molecular mass estimate of 66 kDa, demonstrating that this region of ACC does not contain motifs sufficient for multimerization.

Although BC subunits from prokaryotic ACCs are capable of catalysing biotin carboxylation using free biotin as a substrate [1], it was not clear whether an isolated eukaryotic BC domain would catalyse this reaction, since there was no precedent for it in the literature. We established the appropriate assay using the *E. coli* BC subunit as a positive control, but were unable to detect activity when using rBC (results not shown). The lack of rBC activity towards free biotin may be an intrinsic property of eukaryotic BCs. Alternatively, since the activity of *E. coli* BC requires a homodimer of two functional subunits [24], the lack of rBC activity may be a result of its monomeric structure.

To confirm a native structure in the absence of enzymic activity, rBC was tested in the [^{3}H]soraphen saturation binding assay, and a K_d of 1.1 ± 0.3 nM was determined (mean $\pm$ S.D., $n = 4$; a representative experiment is shown in Figure 4B). This critical result demonstrates that rBC has a native conformation, since it binds soraphen with the same high affinity as both rACC and endogenous *U. maydis* ACC. As an additional negative control for this experiment, *E. coli* BC, the activity of which is not inhibited by soraphen, showed no soraphen binding (Figure 4B).

We next determined the soraphen off-rate by following [^{3}H]soraphen dissociation from rBC. This experiment yielded an estimate for k_{off} of $1.08 \times 10^{-3} \cdot s^{-1}$, corresponding to a dissociation half-life of 10.7 min (results not shown). Note that our binding assays require a separation step that takes 2–3 min, during which time 12–18 % of bound soraphen would dissociate. This would

lead to underestimates of maximum bound ligand, but would have no significant effect on K_d estimates. From the measured k_{off} and K_d values, we can calculate the association rate constant, k_{on}, to be 9.8×10^5 $M^{-1} \cdot s^{-1}$.

Finally, in addition to demonstrating a native conformation, we determined that rBC preparations were very stable, with no loss of soraphen binding or proteolysis detectable for $\geqslant 2$ days at room temperature, $\geqslant 2$ weeks at 4 °C and $\geqslant 6$ months at -20 °C.

Additional BC domains

On the basis of sequence similarity to the region of the *U. maydis* ACC encoded by pCS8, we were able to additionally express BC domains from the ACCs of *M. grisea* and *P. infestans* (i.e. $rBC_{M.g.}$ and $rBC_{P.i.}$). Both $rBC_{M.g.}$ and $rBC_{P.i.}$ were expressed as soluble, His_6-tagged monomers, and the purified products exhibited K_d values for soraphen binding of 0.4 nM and 0.7 nM respectively (results not shown). These results demonstrate our ability to isolate and express functional BC domains from diverse eukaryotic organisms (the pair-wise amino acid identities among the three BC domains ranged from 53–69 %).

Summary

We have cloned, expressed, purified and characterized full-length ACC from the fungus *U. maydis*. The recombinant enzyme exhibited similar substrate kinetics and soraphen binding as the endogenous enzyme. We additionally isolated and expressed truncated BC domains that retain native soraphen binding properties. Together, these reagents will be particularly useful for structural studies, and for the development of assays to screen for novel inhibitors that interact with the soraphen-binding site. Efforts towards these goals are currently under way.

We thank Dr Bridey Maxwell for a critical reading of this manuscript.

REFERENCES

1 Cronan, Jr, J. E. and Waldrop, G. L. (2002) Multi-subunit acetyl-CoA carboxylases. Prog. Lipid Res. **41**, 407–435
2 Toh, H., Kondo, H. and Tanabe, T. (1993) Molecular evolution of biotin-dependent carboxylases. Eur. J. Biochem. **215**, 687–696
3 Nikolau, B. J., Ohlrogge, J. B. and Wurtele, E. S. (2003) Plant biotin-containing carboxylases. Arch. Biochem. Biophys. **414**, 211–222
4 Pridzun, L., Sasse, F. and Reichenbach, H. (1995) Inhibition of fungal acetyl-CoA carboxylase: a novel target discovered with the myxobacterial compound soraphen. In Antifungal Agents: Discovery and Mode of Action (Dixon, G. K., Copping, L. G. and Hollomon, D., eds.), pp. 99–109, Bios Scientific, Oxford
5 Vahlensieck, H. F., Pridzun, L., Reichenbach, H. and Hinnen, A. (1994) Identification of the yeast ACC1 gene product (acetyl-CoA carboxylase) as the target of the polyketide fungicide soraphen A. Curr. Genet. **25**, 95–100
6 Vahlensieck, H.-F. and Hinnen, A. (1997) U.S. Patent 5,641,666
7 Behrbohm, H. (1996) Acetyl-CoA carboxylase from *Ustilago maydis*: purification, characterization, and investigation of inhibition by soraphen A. PhD Thesis, Technical University of Braunschweig
8 Abu-Elheiga, L., Matzuk, M. M., Abo-Hashema, K. A. and Wakil, S. J. (2001) Continuous fatty acid oxidation and reduced fat storage in mice lacking acetyl-CoA carboxylase 2. Science **291**, 2613–2616
9 Abu-Elheiga, L., Oh, W., Kordari, P. and Wakil, S. J. (2003) Acetyl-CoA carboxylase 2 mutant mice are protected against obesity and diabetes induced by high-fat/high-carbohydrate diets. Proc. Natl. Acad. Sci. U.S.A. **100**, 10207–10212
10 Lenhard, J. M. and Gottschalk, W. K. (2002) Preclinical developments in type 2 diabetes. Adv. Drug Deliv. Rev. **54**, 1199–1212
11 Jelenska, J., Sirikhachornkit, A., Haselkorn, R. and Gornicki, P. (2002) The carboxyltransferase activity of the apicoplast acetyl-CoA carboxylase of *Toxoplasma gondii* is the target of aryloxyphenoxypropionate inhibitors. J. Biol. Chem. **277**, 23208–23215
12 Zhang, H., Yang, Z., Shen, Y. and Tong, L. (2003) Crystal structure of the carboxyltransferase domain of acetyl-coenzyme A carboxylase. Science **299**, 2064–2067
13 Kronstad, J. W. and Leong, S. A. (1989) Isolation of two alleles of the b locus of *Ustilago maydis*. Proc. Natl. Acad. Sci. U.S.A. **86**, 978–982
14 Leung, H., Borromeo, E. S., Bernardo, M. A. and Notteghem, J.-L. (1988) Genetic analysis of virulence in the rice blast fungus *Magnaporthe grisea*. Phytopathology **78**, 1227–1233
15 Incledon, B. J. and Hall, J. C. (1997) Evidence that maize acetyl-coenzyme A carboxylase does not function solely as a homodimer. J. Agric. Food Chem. **45**, 4838–4844
16 Matsuhashi, M. (1969) Acetyl-CoA carboxylase from yeast. Methods Enzymol. **14**, 3–8
17 Motulsky, H. J. (1999) GraphPad Software, Inc., San Diego, CA
18 Williams, J. W. and Morrison, J. F. (1979) The kinetics of reversible tight-binding inhibition. Methods Enzymol. **63**, 437–467
19 Kuzmic, P., Elrod, K. C., Cregar, L. M., Sideris, S., Rai, R. and Janc, J. W. (2000) High-throughput screening of enzyme inhibitors: simultaneous determination of tight-binding inhibition constants and enzyme concentration. Anal. Biochem. **286**, 45–50
20 Sumper, M. (1981) Acetyl-CoA carboxylase from yeast. Methods Enzymol. **71**, 34–44
21 Beaty, N. B. and Lane, M. D. (1983) Kinetics of activation of acetyl-CoA carboxylase by citrate. Relationship to the rate of polymerization of the enzyme. J. Biol. Chem. **258**, 13043–13050
22 Munday, M. R. (2002) Regulation of mammalian acetyl-CoA carboxylase. Biochem. Soc. Trans. **30**, 1059–1064
23 Mishina, M., Kamiryo, T. and Numa, S. (1981) Acetyl-CoA carboxylase from *Candida lipolytica*. Methods Enzymol. **71**, 37–44
24 Janiyani, K., Bordelon, T., Waldrop, G. L. and Cronan, Jr, J. E. (2001) Function of *Escherichia coli* biotin carboxylase requires catalytic activity of both subunits of the homodimer. J. Biol. Chem. **276**, 29864–29870

Received 19 December 2003/27 January 2004; accepted 9 February 2004
Published as BJ Immediate Publication 9 February 2004, DOI 10.1042/BJ20031960